# Lawrence Berkeley National Laboratory
## LBL Publications

**Title**
EVIDENCE FOR THE FORMATION OF STABLE ALKYLIDYNE STRUCTURES FROM C3 AND C4 UNSATURATED HYDROCARBONS ADSORBED ON THE Pt(lll) SINGLE CRYSTAL SURFACE

**Permalink**
https://escholarship.org/uc/item/8gd9h9ps

**Author**
Koestner, R.J.

**Publication Date**
1981-08-01

# Lawrence Berkeley Laboratory

## UNIVERSITY OF CALIFORNIA
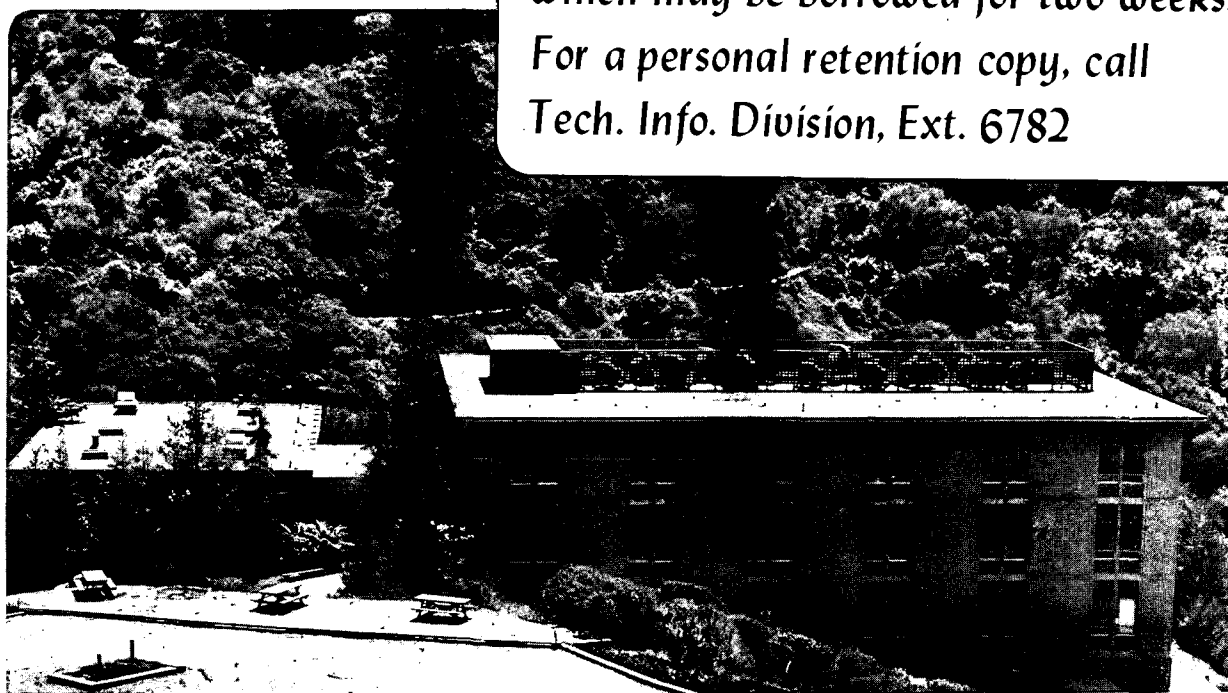
## Materials & Molecular Research Division

EVIDENCE FOR THE FORMATION OF STABLE ALKYLIDYNE STRUCTURES
FROM $C_3$ AND $C_4$ UNSATURATED HYDROCARBONS ADSORBED ON THE
Pt(111) SINGLE CRYSTAL SURFACE

R.J. Koestner, J.C. Frost, P.C. Stair,
M.A. Van Hove, and G.A. Somorjai

August 1981

## DISCLAIMER

# EVIDENCE FOR THE FORMATION OF STABLE ALKYLIDYNE STRUCTURES

## FROM $C_3$ AND $C_4$ UNSATURATED HYDROCARBONS

## ADSORBED ON THE Pt(111) SINGLE CRYSTAL SURFACE

R.J. Koestner, J.C. Frost*, P.C. Stair**, M.A. Van Hove, and G.A. Somorjai

Materials and Molecular Research Division, Lawrence Berkeley Laboratory,
and
Department of Chemistry, University of California, Berkeley, CA 94720

## Abstract

$C_3$ and $C_4$ hydrocarbon (methylacetylene, propylene, and the 2-butenes) adsorption on the Pt(111) face was studied by observing the LEED patterns that formed and by measuring the intensity vs. voltage spectra for each structure. Two phases exist for each of these molecules adsorbed on the Pt(111) surface. At low temperatures, the unsaturated C-C group forms a di-$\sigma$ bond to two Pt atoms. Upon warming to about room temperature, and in the presence of hydrogen for the alkynes, a conversion takes place to an alkylidyne species that is bonded to three Pt atoms and has its C-C bond nearest to the metal substrate oriented perpendicularly to the surface. The butylidyne species is shown to order its ethyl group into an (8x8) or $(2\sqrt{3}x2\sqrt{3})R30°$ superlattice when the hydrocarbon exposure is increased; this ordering is probably a natural consequence of the steric hindrance among neighboring ethyl groups as the hydrocarbon coverage increases slightly with larger exposures.

*Permanent address: Dept. of Chemistry, Heriot-Watt University, Riccarton, Currie, Edinburgh, Scotland.

**Permanent address: Dept. of Chemistry and Materials Research Center, Northwestern University, Evanston, IL 60201.

Introduction

The structure of adsorbed monolayers of unsaturated hydrocarbons on platinum single crystal surfaces has been the subject of intense investigations by a variety of techniques over the last several years. For the most part, these studies concentrated on the structure of acetylene and ethylene adsorbed on the Pt(111) face as a function of temperature. A clear picture is now emerging on the bonding of these simple hydrocarbons to the Pt(111) surface. Below room temperature, both acetylene and ethylene have been proposed to be di σ bonded to two Pt atoms and have their carbon-carbon bond parallel to the surface; however, only acetylene forms an ordered overlayer (with a diffraction pattern corresponding to a (2x2) surface structure). Figure 1 shows the model proposed for this metastable, low temperature acetylene phase on the basis of high resolution electron energy loss spectroscopy (HREELS)[1,2] and ultraviolet photoemission spectroscopy (UPS)[3,4] studies; acetylene is thought to be roughly $sp^2$ hybridized and may have some additional π bonding to a third metal atom that tilts the molecular plane away from the surface normal. The metastable, low temperature ethylene species is probably di σ bonded to two Pt atoms and $sp^3$ hybridized [1,3,4].

In the temperature range of about 350-450 K, the low temperature acetylene phase transforms irreversibly into vinylidene ($=C=CH_2$) in the absence of coadsorbed hydrogen and into ethylidyne ($\equiv C-CH_3$) in the presence of coadsorbed hydrogen. Evidence for the vinylidene transition comes from UPS [5] and HREELS studies [1], and from the existence of similar reactions in organometallic chemistry [6]; the transition to ethylidyne was first proposed by a dynamical low energy electron diffraction (LEED) analysis [7]. This transition to ethylidyne is an order-order transformation of (2x2)->(2x2) surface structures, while it is not known whether the transition to vinylidene gives an ordered surface structure. In addition to

the ethylidyne model, early HREELS work (1] suggested an ethylidene (=CHCH$_3$)

species and UPS studies [5] indicated a vinyl-like (=CH-CH$_2$-) species (better

named 1-ethanyl-2-ylidene). Recently, however, the ethylidyne species (see

Fig.2) has gained acceptance over the competing models partly as a consequence

of a normal mode analysis [8] of the IR spectrum for an organometallic analogue

Co$_3$(CCH$_3$)(CO)$_9$ that shows excellent agreement with the ethylidyne model's vibra-

tional peak assignment for the original HREELS spectrum [1]. Further, the C$_2$H$_3$

stoichiometry of ethylidyne was measured for the ethylene overlayer from a com-

bined UPS and thermal desorption spectroscopy (TDS) study [5], while an angle-

resolved UPS study [10] also indicated the presence of an ethylidyne species.

The low temperature ethylene phase was similarly observed to make an irre-

versible transition to an ethylidyne species at 280 K since the resulting

LEED pattern, I-V profiles [9], HREELS spectra [1], and UPS spectra [11] are

identical to those obtained from the stable, hydrogen-treated acetylene overlayer.

Finally, both acetylene and ethylene above ~450 K have been seen by HREELS

[12] to fragment into smaller hydrocarbon species ($\equiv$ CH,=CH$_2$).

These studies reveal the rich diversity and temperature dependent char-

acter of the surface chemical bond of organic molecules. It is our aim, by

systematic studies of the structure of small hydrocarbon molecules on transition

metal surfaces, to uncover the dominant bonding characteristics common to

this family of adsorbed molecules. For this reason we have studied and report

in this paper the structure of ordered monolayers of propylene, methylacetylene,

and the cis- and trans-2-butenes adsorbed on the Pt(111) face. We present inter-

pretations of both the observed LEED patterns and the large set of intensity

vs. energy (I-V) curves obtained for these molecules. In this way we aim to

demonstrate that these larger, unsaturated hydrocarbons bond to the Pt(111)

face in a way very similar to acetylene and ethylene by forming alkylidyne

($\equiv$ C-(CH$_2$)$_n$-CH$_3$) species at room temperature. Specifically, the C$_3$ and C$_4$
structures can be obtained by substituting methyl groups for single hydrogens of
the C$_2$ and C$_3$ alkylidyne species, respectively. Table I summarizes our
models for C$_2$, C$_3$, and C$_4$ hydrocarbon adsorption on the Pt(111) surface;
this table is included to aid in following the discussion below by exhibiting
the relationship among various structures.

Convincing additional evidence for our proposed alkylidyne structure on the
Pt(111) comes from similar HREELS [13] and LEED [14] experiments being performed
for the same hydrocarbon molecules adsorbed on a different metal surface,
Rh(111), where a very similar sequence of LEED patterns and I-V curves occurs.

Experimental

The different hydrocarbon gases used were obtained from the Matheson
Company, except for methylacetylene which was purchased from Air Products
Corporation. Methylacetylene was found to contain 5% acetylene by gas chromo-
tography so the gas sample was first pumped at dry ice temperatures to reduce the
acetylene contamination to about 0.1%. Propylene had only a 0.2% impurity of
ethane and methane as well as 0.05% acetylene, and therefore was introduced
into the vacuum chamber without further purification. The cis- and trans-2-
butenes were nominally 95% pure (with the major impurity being the other isomer),
but were also used without further purification. The Pt sample was purchased
from Materials Research Corporation and has a nominal 1 ppm impurity level.
The crystal was oriented and spark cut to within 0.5° of the (111) plane using
back-diffraction Laue. The crystal was then polished by emery papers and a
0.5 $\mu$ m diamond paste before insertion into the UHV chamber.

The C$_3$ and C$_4$ hydrocarbon adsorption experiments were carried out in two
different vacuum chambers; each was equipped with retarding-field Auger electron

spectrocopy, a Varian ion sputtering gun, a Varian off-axis LEED gun, a UTI quadrupole mass spectrometer, and a modified Varian manipulator allowing azimuthal and polar rotations. The base pressure of both chambers was maintained at $\sim 1 \times 10^{-9}$ torr. The I-V curves were measured using a photographic technique already described [15]. The photographs of the LEED spot pattern, taken at 2 eV intervals, were digitized with a scanning microdensitometer; the resulting density map at successive energies were translated with a new computer program into the desired intensity-energy (I-V) profiles.

The Pt sample was cleaned of calcium, phosphorus, and carbon by a combination of oxygen treatments ($5 \times 10^{-7}$ torr $O_2$, 10 minutes, 700°C with a subsequent flash to 1000°C) and Ar ion bombardments (with subsequent 800°C annealing for 5 minutes). Ar ion bombardments would not leave any contaminating carbon on the surface after a series of 1-2 L hydrocarbon exposures; however, after the 100-1000 L exposures, oxygen treatments were necessary to effectively remove the carbon. The sample was flashed just before the hydrocarbon exposures to remove any pre-adsorbed carbon monoxide; yet about 0.05 monolayers of carbon monoxide would coadsorb with each hydrocarbon during exposure due to the displacement of carbon monoxide from the chamber wall.

Results

A. LEED Patterns

The clean platinum (111) crystal face was held at 300 K while it was exposed to the different hydrocarbons. A 1-2 L exposure (1 L= $10^{-6}$ torr sec) to methylacetylene or propylene was sufficient to produce a well ordered (2x2) surface structure with sharp diffraction beams. It was found that overexposure to either organic vapor would not reduce the quality of the LEED pattern, whereas only a 10% overexposure to acetylene in previous

studies would cause a noticeable disordering of the adsorbed layer [9]. Both $C_3$ hydrocarbons ordered spontaneously upon adsorption, unlike ethylene that ordered well only when exposed to the electron beam [9]. The $C_3$ adsorbates showed a 50% higher carbon coverage than the $C_2$ overlayers by Auger electron spectroscopy (AES).

Only one ordered phase of propylene was found by the inspection of the I-V curves from its (2x2) surface structure in the temperature range of 280-400 K. Below 280 K a poor (1x1) LEED pattern is obtained that is indicative of disordered propylene adsorption. The methylacetylene that also adsorbs in a (2x2) surface structure makes an order-order transition [(2x2)metastable-->(2x2)stable] in the presence of background hydrogen after one hour at 350-400 K or after ~24 hours at 300 K as determined by monitoring the I-V curves . The (2x2) surface structures of both $C_3$ hydrocarbons would disorder at around 400 K similar to the behavior of the $C_2$ hydrocarbons adsorbed on Pt(111).

The cis- and trans-2-butenes were admitted into the chamber at low ( ~ 10 L), intermediate ( ~ 100 L), and high ( ~ 1000 L) exposures. For even the lowest exposures (~ 1/4 L), a $(2\sqrt{3}x2\sqrt{3})R30°$ surface structure was observed. The half-order spots of this very low exposure pattern, i.e. those already present in the diffraction pattern of a (2x2) unit cell, had gained substantial intensity and were fairly well focused, while the remaining spots (those in addition to the half-order and integral-order spots) were very diffuse and weak in intensity. Upon increasing the exposure to ~10 L, the half-order spots would reach near-maximum intensity, though the remaining sixth-order spots did not become comparably strong and sharp until an exposure of ~1000 L had been reached. At intermediate exposures above ~ 1000 L, a well-ordered LEED pattern corresponding to an (8x8) surface structure would sometimes form, while at other times the $(2\sqrt{3}x2\sqrt{3})R30°$ structure would continue to appear with the sixth-order beams

becoming gradually more intense and better focussed as the hydrocarbon exposure approached 1000 L. When the (8x8) phase did form, it could easily transform into the $(2\sqrt{3}x2\sqrt{3})R30°$ structure with incrasing exposure. Figure 3 shows the LEED patterns associated with (a) the stable propylene (2x2) structure, (b) the (2x2) structure of the 2-butenes formed at ~10 L, (c) the $(2\sqrt{3}x2\sqrt{3})R30°$ -2-butene overlayer at ~1000 L, and (d) the (8x8) -2-butene structure seen at ~ 100 L.

The cis- and trans-2-butenes did not give an ordered LEED pattern below about 280 K, while the ordered, room temperature phases [$(2\sqrt{3}x2\sqrt{3})R30°$ and (8x8)] would disorder at ~325 K. Interestingly, the half- and integral-order spot intensities would not fade as quickly as those from the remaining spots in the $(2\sqrt{3}x2\sqrt{3})R30°$ and (8x8) overlayers when the temperature or the electron beam exposure is increased. Thus the gradual emergence of a well-ordered $(2\sqrt{3}x2\sqrt{3})R30°$ surface strucutre with increasing hydrocarbon exposure as well as the delicate nature of the sixth- or eight-order spots with increasing temperature or LEED beam exposure suggests the presence of a $(2\sqrt{3}x2\sqrt{3})R30°$ superlattice in superimposed on the usual (2x2) lattice of hydrocarbon adsorption sites.

B.  Comparison of I-V Curves

The I-V spectra for metastable methylacetylene (28 independent beams), stable methylacetylene (28 independent beams), and propylene (26 independent beams) at five angles of incidence ($\theta$=0,4,8,10,16°; $\phi$=0°) were obtained and are available at request either in digitized form or as plotted curves. A smaller data base of only normal incidence curves ($\theta$=0°, 4-7 independent beams) was obtained for the $(2\sqrt{3}x2\sqrt{3})R30°$ cis-2-butene and trans-2-butene, and (8x8) trans-2-butene structures; these $C_4$ spectra are also available on request. In this paper we show several I-V curves that may be taken as representative of the available much larger data base.

There are many identities and similarities to be found in the diffraction

data obtained for the different hydrocarbons studied. We would like to call attention to four important findings: (1) Fig.4 illustrates the similarity between I-V curves obtained for the metastable methylacetylene and acetylene structures. (2) Figs.5 and 6 show that the stable phases of acetylene, ethylene, methylacetylene, and propylene have nearly identical I-V curves except for a few systematic and reproducible differences which occur between the curves for $C_2$ hydrocarbons and $C_3$ hydrocarbons. (3) We compare in Fig.7 the low exposure ( ~10 L) (2x2) cis-2-butene I-V curves to both the high exposure ( ~ 1000 L) (2 $\sqrt{3}$x2 $\sqrt{3}$)R30° cis- or trans-2-butene and the (2x2) propylene curves. The spectra for the (2x2) cis-2-butene structure are intermediate between those for (2x2) propylene and those for (2 $\sqrt{3}$x2 $\sqrt{3}$)R30° cis- or trans-2-butene, while the latter two structures produce rather different I-V spectra. This comparison of I-V curves indicates that when the extra diffraction beams from the (2 $\sqrt{3}$x2 $\sqrt{3}$)R30° structure of the $C_4$ hydrocarbon overlayer are very weak in intensity and diffuse, the half-order intensity spectra are very similar for all the $C_2$, $C_3$, and $C_4$ hydrocarbon overlayers. But once the (2 $\sqrt{3}$x2 $\sqrt{3}$)R30° surface pattern is fully developed, the half-order intensity curves for the $C_2$ or $C_3$ hydrocarbons and the $C_4$ hydrocarbons diverge. (4) We compare in Fig.8 some common I-V profiles for the high exposure (2 $\sqrt{3}$x2 $\sqrt{3}$)R30° cis- and trans-2-butene as well as the intermediate exposure (8x8) trans-2-butene structures. The three sets of common I-V spectra are seen to be identical within experimental error, indicating the cis and trans isomers form the same overlayer structure, as well as showing that the (8x8) trans-2-butene overlayer geometry must be very similar to that of the (2 $\sqrt{3}$x2 $\sqrt{3}$)R30° surface structure.

Discussion

The similarity or virtual identity of the $C_2$, $C_3$, and $C_4$ hydrocarbon I-V

spectra indicate the structural similarity of the adsorbed species. The geometric location, bond distances, and orientation of that part of the carbon skeleton in each molecule ($\equiv$C-CH$_2$R or H$_2$C=CHR) that is responsible for anchoring it to the platinum surface in an ordered structure is the same from adsorbate to adsorbate. The very similar progression of LEED patterns for these adsorbed species with increasing temperature further indicates the similarity in both their structure and their intramolecular rearrangement during the metastable to stable phase transition.

The similarity of the temperature dependent structural reorganization is also demonstrated in a recent thermal desorption study (TDS) [16] of these molecules as can be seen in Fig.9. The desorption of hydrogen is monitored from the adsorbed monolayers of the alkenes on the Pt(111) crystal face. The peaks indicate the maximum rates of desorption. The adsorbed layers dehydrogenate sequentially with increasing temperature in a very similar manner. Peaks A and C are found in all the desorption traces for ethylene, propylene, and the 2-butenes, while peak B shifts to lower temperature with the longer chain hydrocarbons. Peak A is assigned to partial dehydrogenation of the alkene by removal of one hydrogen in the conversion from a parallel bonded, metastable species to a stable species. Peak B corresponds to C-C bond scission and fragmentation of the hydrocarbons, and peaks C probably represent the final dehydrogenation of the small hydrocarbon fragments left on the platinum surface. It is important to note that the adsorbed hydrocarbons do not (at peak A) decompose into the species that the smaller hydrocarbons adopt; this indicates that the larger adsorbed hydrocarbons retain their gas-phase carbon skeleton at room temperature.

Let us now address the question why certain diffraction beam intensities from the ordered overlayers of the $C_2$, $C_3$, an $C_4$ hydrocarbons remain unaltered. A perfectly disordered set of adsorbed atoms on an otherwise well ordered surface

contributes a negligible amount to the LEED beam intensities since the diffraction
by a disordered layer is diffuse in space. If that layer gradually orders
into a certain lattice, the contribution by that layer to beams defined by its
reciprocal lattice grows. As a result, existing I-V curves can be strongly
affected if the scattering strength of the newly ordered atoms is significant.
Thus our observations of a $(2\sqrt{3}\times2\sqrt{3})R30°$ surface structure developing from
a (2x2) structure with gradual changes in the I-V curves from the (2x2) structure
indicate that atoms which were disordered, are ordering into a $(2\sqrt{3}\times2\sqrt{3})R30°$
lattice; at the same time the other atoms responsible for the ordered (2x2)
structure are very little affected by this new ordering process.

We shall now discuss the proposed structures for each adsorbate (methyl-
acetylene, propylene, and the 2-butenes). These surface structures are also
summarized in Table I.

### A. Metastable Methylacetylene ($H_3C-C\equiv CH$).

We interpret the virtual identity of the metastable acetylene and
methylacetylene I-V spectra shown in Fig.4 as follows: Replacing a hydrogen
atom of the adsorbed $C_2H_2$ species by a methyl group produces the structure
of adsorbed methylacetylene, if one assumes a randomness in the choice of
the hydrogen atom or a randomness in the orientation of the methyl group.
The probable $sp^2$ rehybridization of methylacetylene twists the methyl group
away from the surface, thereby giving it the necessary space to rotate more
freely. Fig.10 illustrates our proposed geometry for the metastable methyl-
acetylene species.

### B. Stable Propylene ($CH_3-CH=CH$)

Between 280 K and the decomposition temperature of 400 K, the I-V
spectra for propylene and ethylene are nearly identical, as can be seen in Figs.
5 and 6. This can be interpreted to imply that the room temperature propylene
species has a structure like that of the room temperature ethylene except
that one of the ethylidyne hydrogens is replaced by a methyl group that is ro-
tationally disordered. This model, consisting of a propylidyne species, is
illustrated in Fig.11. Using standard Van der Waals atomic radii, we find
that neighboring molecules nearly touch in this structure. In fact, some rela-
tive orientations of neighboring methyl groups are sterically not possible, but

enough rotational freedom is left to explain the virtual identity of I-V curves
mentioned above. These steric considerations are also consistent with the
observed spontaneous ordering of the stable propylene molecules, contrasting
with the non-spontaneous ordering of the smaller stable ethylene molecules that
require exposure to the electron beam. Furthermore, a 50% overexposure of pro-
pylene or methylacetylene does not disorder the (2x2) LEED pattern, whereas it
does with ethylene or acetylene; this should be expected since there would
be less interstitial adsorption due to the $C_3$ hydrocarbons' larger size.

C. Stable Methylacetylene ($CH_3-C{\equiv}CH$)

Methylacetylene like acetylene shows a hydrogen assisted order-order
transformation to form a stable (2x2) overlayer at 300-350 K. The stable
structure I-V curves (Figs.5,6) are nearly identical to those for the room
temperature ethylene, acetylene, and propylene phases. This, together with
the intactness of the carbon skeleton, demonstrates that the parallel bonded
$sp^2$ hybridized methylacetylene transforms in the presence of additional hydrogen
into the same propylidyne species that propylene does (Fig.11).

D. Low (~10 L) and High (~1000 L) Exposure 2-butenes ($CH_3-CH=CH-CH_3$)

The cis- and trans-2-butenes gave identical $(2\sqrt{3}x2\sqrt{3})R30°$ I-V
profiles in Fig.8 and have been shown to yield identical TDS spectra [16]. This
indicates that both isomers form the same surface structure so that we can ignore
their different molecular origin in the following discussion.

At even the lowest 2-butene exposures (~1/4 L) tried, a LEED pattern
corresponding to a $(2\sqrt{3}x2\sqrt{3})R30°$ unit cell was observed with poorly developed
extra spots, i.e. those in addition to the half-order and integral-order ones,
In Fig. 7 we saw that the half-order I-V profiles for the low exposure
2-butene phase seem intermediate between the stable propylene spectra and the
2-butene curves from the well developed $(2\sqrt{3}x2\sqrt{3})R30°$ structure. This
suggests that the low exposure structure consists of a butylidyne species

($\equiv$ C-CH$_2$-CH$_2$-CH$_3$) with a partially disordered ethyl group (-CH$_2$-CH$_3$), while the high exposure structure consists of a butylidyne species with the ethyl group ordered into a (2 $\sqrt{3}$x2 $\sqrt{3}$)R30° unit cell.

From a parallel study [14], propylene adsorbed on the Rh(111) surface is shown to behave very much like the 2-butenes on Pt(111) by forming a low exposure (2x2) and, at higher exposures, a (2 $\sqrt{3}$x2 $\sqrt{3}$)R30° surface structure. In fact, the half-order diffraction beam I-V curves from the low exposure propylene phase on Rh(111) are even more similar to the I-V spectra obtained from the (2x2) ethylene structure than for the corresponding low exposure 2-butene intensity spectra on Pt(111). This observation is to be expected since the partially ordered ethyl group (-CH$_2$-CH$_3$) of butylidyne ($\equiv$C-(CH$_2$)$_2$-CH$_3$) has a larger scattering strength than the methyl group (-CH$_3$) of propylidyne ($\equiv$C-CH$_2$-CH$_3$) and thus should alter the resulting I-V spectra more dramatically.

The appearance of a (2 $\sqrt{3}$x2 $\sqrt{3}$)R30° unit cell is presumably due to the interaction between neighboring ethyl groups in the butylidyne overlayer. A possible structural model is illustrated in Fig. 12. Few other models are compatible with the available experimental evidence. Three butylidyne molecules fit in the unit cell, but are restricted in the orientation of the ethyl groups by mutual steric hindrance. Fig. 12a shows hydrogen atoms with their Van der Waals radii, while Fig. 12b emphasized the hydrocarbon skeleton in the same structure. The neighboring hydrocarbon arms are rotated as far as possible from each other, while the well-known planar zig-zag conformation of the carbon skeleton within each butylidyne species leads to a minimum in the repulsion of non-bonding carbon atoms in the chain. Note that this model places the upper methyl groups in a vertical direction, thus minimizing overlap between these groups on neighboring molecules. We have assumed in Figs. 11 and 12 a "staggered" rather

tha "eclipsed" bonding arrangement about the two carbon atoms closest to the metal surface, paralleling the lowest energy conformation of ethane. The exact bond lenths and angles in the ethyl groups can only be determined by a detailed analysis of the I-V curves which would also test the correctness of our structural model. Such an analysis is in progress.

Finally, we note that the butylidene [=CH-(CH$_2$)$_2$-CH$_3$] or 1-butanyl-2-lidene [=CH-CH(CH$_2$CH$_3$)-] species cannot be as easily packed into the (2x√3x2√3)R30° unit cell; this, then, provides further support for ethylidyne (≡C-CH$_3$) over ethylidene (=CH-CH$_3$) or 1-ethanyl-2-ylidene (=CH-CH$_2$-).

Interestingly, a 100-fold higher exposure is needed to adequately order the sixth-order spots than the half-order ones in the diffraction pattern for the (2√3x2√3)R30° structure. It may be that the large hydrocarbons can block neighboring adsorption sites so that only after a period of time would any given butylidyne species conform in such a way to open a neighboring, unoccupied site to an approaching molecule. In this way the saturation coverage is reached only after a fairly long time and only then could the C$_4$ molecules be crowded enough to adequately order into the (2√3x2√3)R30° unit cell. Yet it should be emphasized that we believe a near-saturation coverage is already achieved at 10 L since the half-order spots are very well focused and near maximum intensity.

E. <u>Intermediate Exposure ( ~ 100 L) 2-Butenes</u>

The (8x8) trans-2-butene pattern formed after ~ 100 L exposure at 300 K on the Pt(111) surface; Fig. 8 shows that the common beam profiles between the (8x8) and (2√3x2√3)R30° structures are identical. This indicates that the two phases must have very similar structures, yet we cannot suggest a reasonable model for the (8x8) structure at present.

Summary

Within the range of molecules considered in this paper (ethylene, acetylene, propylene, methylacetylene, and the 2-butenes), the alkenes and alkynes have closely related LEED patterns and I-V spectra. Two phases exist for each of these molecules adsorbed on Pt(111); for each molecule, a low temperature, "metastable" species is parallel bonded to the surface. Upon warming to about room temperature, and in the presence of hydrogen for the alkynes, a conversion takes place to an alkylidyne species that is bonded to three platinum atoms and has its C-C bond nearest to the metal substrate oriented perpendicularly to the surface. Table I summarizes the different surface structures proposed for the $C_2, C_3$, and $C_4$ hydrocarbons considered.

Though a LEED analysis should be undertaken to confirm our proposed butylidyne structure, convincing evidence is already contained in the similarity of the I-V spectra, in the Van der Waals models of these large, close packed hydrocarbons, in the gradual development of a $(2\sqrt{3} \times 2\sqrt{3})R30°$ LEED pattern with increasing exposure, and in the correlations among $C_2$, $C_3$, $C_4$ hydrocarbon TDS spectra. We show that the LEED pattern comes about by having the ethyl group of the butylidyne species begin to order into a $(2\sqrt{3} \times 2\sqrt{3})R30°$ unit cell, while the two carbon atoms of the $C_4$ molecule that are nearest the metal remain in positions that are identical to those occupied in the ethylidyne species with a (2x2) unit cell. We further show that the model of the alkylidyne surface species agrees with the experimental evidence much better than other models such as alkylidene or 1-alkanyl-2-ylidene. Of interest also is a parallel sequence of very similar structures found for $C_2$ and $C_3$ hydrocarbons on Rh(111).

Finally, we suggest that the intermediate exposure (8x8) 2-butene structure may also consist of a butylidyne species. Yet more experiments are needed to elucidate this structure.

-------------

## Acknowledgement

## References

1.  H. Ibach, S. Lehwald, J. Vac. Sci. & Technol. 15, 407 (1978).

2.  H. Ibach, H. Hopster, B. Sexton, Appl. Phys. 14, 21 (1977).

3.  J.E. Demuth, Surface Sci. 84, 315 (1979).

4.  T.E. Felter and W.H. Weinberg, Surface Sci. 103, 265 (1981).

5.  J.E. Demuth, Surface Sci. 80, 367 (1979).

6a. A.J. Deeming, M. Underhill, J.C.S. Dalton, 1415 (1974).

6b. A.J. Deeming, M. Underhill, J.C.S. Dalton, 1614, (1975).

7.  L.L. Kesmodel, L. H. Dubois, and G.A. Somorjai, J. Chem. Phys. 70, 2180 (1979).

8.  P. Skinner, M.W. Howard, I.A. Oxton, S.F.A. Kettle, D.P. Powell, and N. Sheppard (to be published), 1981.

9.  P.C. Stair and G.A. Somorjai, J. Chem. Phys. 66, 2036 (1977).

10. M.R. Albert, L.G. Sneddon, E.W. Plummer, T. Gustafsson, ACS annual meeting, New York, NY, 1981.

11. W.-J. Lo, Y.-W. Chung, L.L. Kesmodel, P.C. Stair, and G.A. Somorjai, Solid State Comm. 22, 335 (1977).

12. A.M. Baro, H. Ibach, J. Chem. Phys. in press.

13. L.H. Dubois, D.G. Castner, and G.A. Somorjai, J. Chem. Phys. 72, 5234 (1980).

14. R.J. Koestner, M.A. Van Hove, and G.A. Somorjai (to be published).

15. P.C. Stair, T.J. Kaminska, L.L. Kesmodel, and G.A. Somorjai, Phys. Rev. B11, 623 (1975).

16. M. Salmeron and G.A. Somorjai, J. Phys. Chem. (to be published), 1981.

Figure Captions

Figure 1.  The metastable acetylene species is shown di-σ bonded to two Pt atoms
with some additional π bonding to a third Pt atom.

Figure 2.  The stable acetylene or ethylene phase forms an ethylidyne species.

Figure 3.  Progression of LEED patterns for the room temperature structures of
the $C_2$, $C_3$, and $C_4$ hydrocarbons.

Figure 4.  Comparison of the I-V curves obtained from the metastable acetylene
and methylacetylene structures.

Figures     Comparison of the I-V curves obtianed from the stable acetylene,
5 and 6.    ethylene, methylacetylene, and propylene phases.

Figure 7.  Comparison of the I-V curves obtained frm the (2x2) propylene, the
low exposure (~10 L) $(2\sqrt{3}x2\sqrt{3})R30°$ 2-butene, and the high exposure
(~1000 L) $(2\sqrt{3}x2\sqrt{3})R30°$ 2-butene phases.

Figure 8.  Comparison of the I-V curves obtained from the high exposure
(~1000 L) $(2\sqrt{3}x2\sqrt{3})R30°$ cis-2-butene, the high exposure (~1000 L)
$(2\sqrt{3}x2\sqrt{3})R30°$ trans-2-butene, and the intermediate (100 L) (8x8)
trans-2-butene structures.

Figure 9.  TDS spectra of ethylene ($C_2H_4$), propylene ($C_3H_6$), and the 2-butenes
($C_4H_8$) adsorbed on Pt(111). (This figure is taken from Ref. 16.)

Figure 10. The metastable methylacetylene species is di σ bonded to two Pt atoms
with some additional π bonding to the third Pt atom.  The methyl group
is presumed randomly attached to either of the two lower carbon atoms.

Figure 11. The stable methylacetylene or propylene phase forms a propylidyne
species, shown here with various methyl orientations.

Figure 12. The 2-butenes form a butylidyne complex on Pt(111), seen here perpen-
dicular to the surface.  The upper sketch shows the Van der Waals
radii of the adsorbed hydrocarbon, while the lower sketch emphasizes
the carbon skeleton.  The $(2\sqrt{3}x2\sqrt{3})R30°$ unit cell containing three
butylidynes is shown.
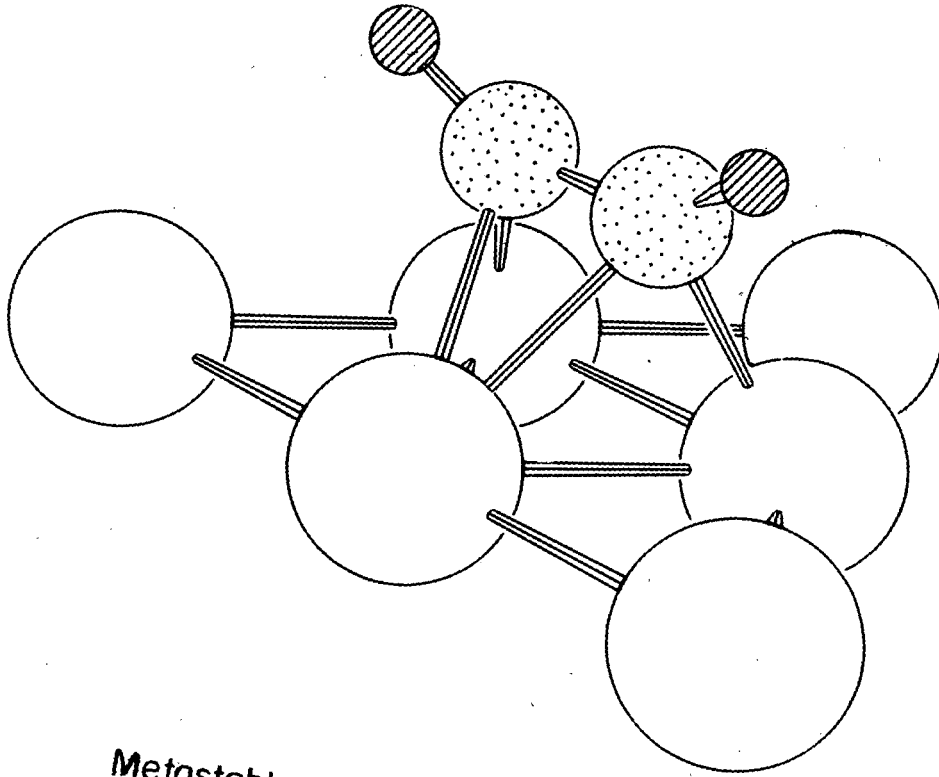
Metastable acetylene on Pt(III)

XBL 817-6066

Fig.1
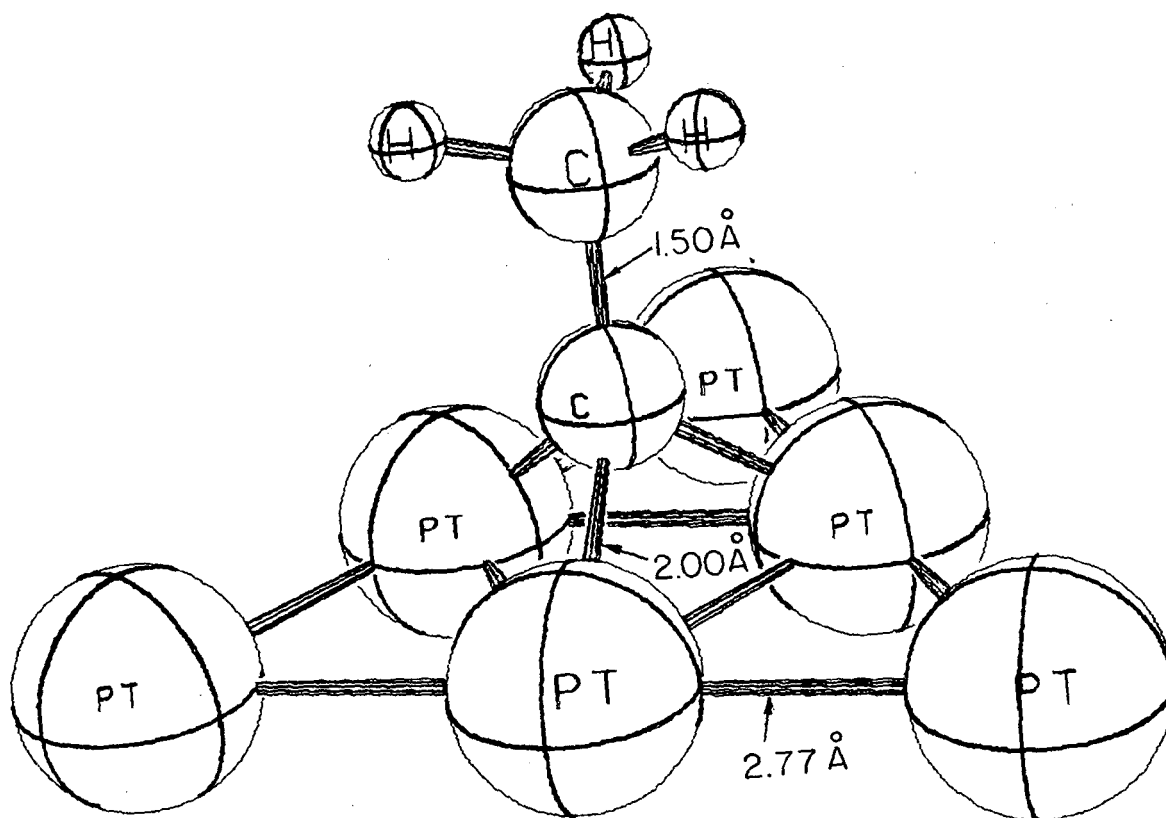
Pt (III) + ethylidyne

XBL794-6167
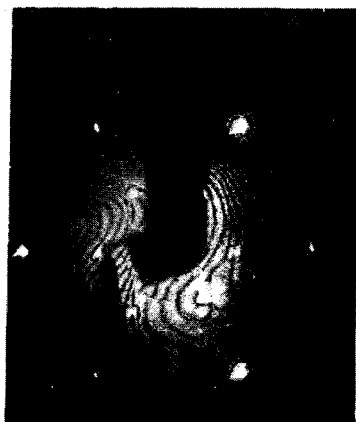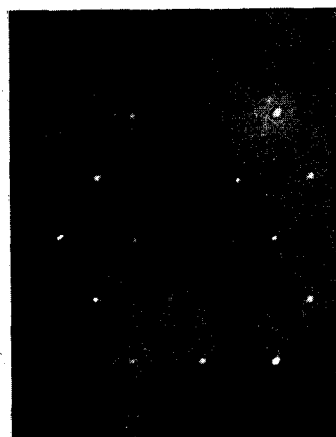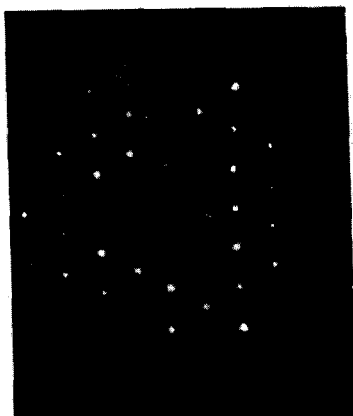
Fig.2

T = 300 K,    $\theta = 0°$,    52 eV



Pt(III) -C$_2$H$_4$ - (2×2)
" -C$_2$H$_2$+H- "
" -C$_3$H$_6$- "
" -C$_3$H$_4$+H- "



Pt(III)-cis-2-C$_4$H$_8$-(2×2)+diffuse (2√3×2√3)R30°



Pt(III)-cis-2-C$_4$H$_8$-(2×2)+(2√3×2√3)R30°
" -trans-2-C$_4$H$_8$- "      "



Pt(III)-trans-2-C$_4$H$_8$-(8×8)

XBB 813-2590

Fig.3

Fig. 4

# METASTABLE STRUCTURE
## T = 300 K

$\theta = 0°$

$(0 \ \bar{1}{2})$

$\times\frac{1}{4}$

$C_2H_2$

$C_3H_4$

$\theta = 16°, \ \phi = 0°$

$(0 \ \bar{1}{2})$

$\times\frac{1}{2}$

$\times\frac{1}{2}$

$C_2H_2$

$C_3H_4$

$\times\frac{1}{4}$

$(\frac{1}{2} \ \bar{1}{2})$

$\times\frac{1}{2}$

$C_2H_2$

$C_3H_4$

$\times\frac{1}{2}$

$(\bar{1}{2} \ 0)$

$\times\frac{1}{2}$

$C_2H_2$

$C_3H_4$

INTENSITY

$(\bar{1}{2} \ \bar{1}{2})$

$C_2H_2$

$C_3H_4$

$(\bar{1}{2} \ \bar{1}{2})$

$C_2H_2$

$C_3H_4$

0    40    80    120    160    200
ENERGY (eV)

0    40    80    120    160    200
ENERGY (eV)

XBL 817-6050

STABLE STRUCTURE-Pt (III)

$\theta = 0°$

T = 300 K

$\left( \frac{\bar{1}}{2} \quad \frac{\bar{1}}{2} \right)$

$\theta = 16°, \quad \phi = 0°$

INTENSITY

$C_2H_2$

$C_2H_4$

$C_3H_4$

$C_3H_6$

ENERGY (eV)

ENERGY (eV)

XBL 7511-7638

Fig. 5

22

23



STABLE STRUCTURE – Pt (III)
T = 300 K

$\theta = 16°, \phi = 0°$

$\theta = 0°$

$(0 \frac{\bar{1}}{2})$

$(\frac{1}{2} \frac{\bar{1}}{2})$

$(\frac{\bar{1}}{2} 0)$

$(0 \frac{\bar{1}}{2})$

INTENSITY

$C_2H_2$

$C_2H_4$

$C_3H_4$

$C_3H_6$

ENERGY (eV)

XBL 817-6064

Fig.6

$\theta = 0°$, T = 300 K

$\left(\frac{1}{2}\ 0\right)$

$\left(\frac{1}{2}\ \frac{1}{2}\right)$

INTENSITY

Pt (III) + (2×2) $C_3H_6$

Pt (III) + (2×2) and
diffuse $(2\sqrt{3} \times 2\sqrt{3})R30°$
cis – 2 – $C_4H_8$

Pt(III) + $(2\sqrt{3} \times 2\sqrt{3})R30°$
cis – 2 – $C_4H_8$

ENERGY (eV)

ENERGY (eV)

XBL 813 - 5396

Fig. 7a

24

Fig. 7b

25

$\theta = 0°$, T = 300 K

$\left(0\ \dfrac{1}{2}\right)$

$\left(0\ 1\right)$

Pt (III) + (2×2) $C_3H_6$

Pt (III) + (2×2) and
diffuse $(2\sqrt{3} \times 2\sqrt{3})R30°$
cis - 2 - $C_4H_8$

Pt (III) + $(2\sqrt{3} \times 2\sqrt{3})R30°$
cis - 2 - $C_4H_8$

INTENSITY

ENERGY (eV)

ENERGY (eV)

XBL8I3-5395

$\theta = 0°$,  T = 300 K

........... Pt (III) + p (8×8) trans-2-$C_4H_8$

----- Pt (III) + $(2\sqrt{3} \times 2\sqrt{3})$R 30° trans-2-$C_4H_8$

——— Pt (III) + $(2\sqrt{3} \times 2\sqrt{3})$R 30° cis-2-$C_4H_8$

$(\frac{1}{2}\ 0)$

$(\frac{1}{2}\ \frac{1}{2})$

$(0\ \frac{1}{2})$

$(0\ 1)$

INTENSITY

eV

eV

Fig. 8

26

XBL 813-5394

27



Fig.9

Methyl group is
randomly attached
to either carbon atom

Metastable methylacetylene on Pt (III)

XBL 817-6067

Fig.10
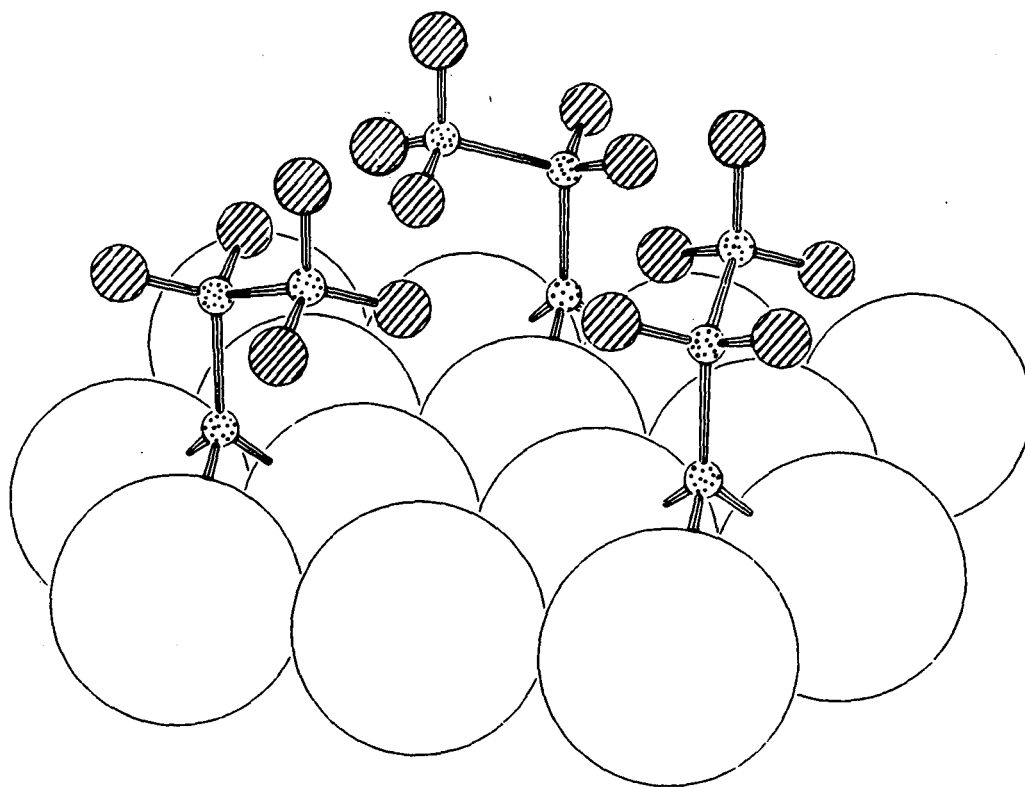
fcc (III) + $C_3H_5$   (propylidyne)

XBL 817- 6065

Fig.11
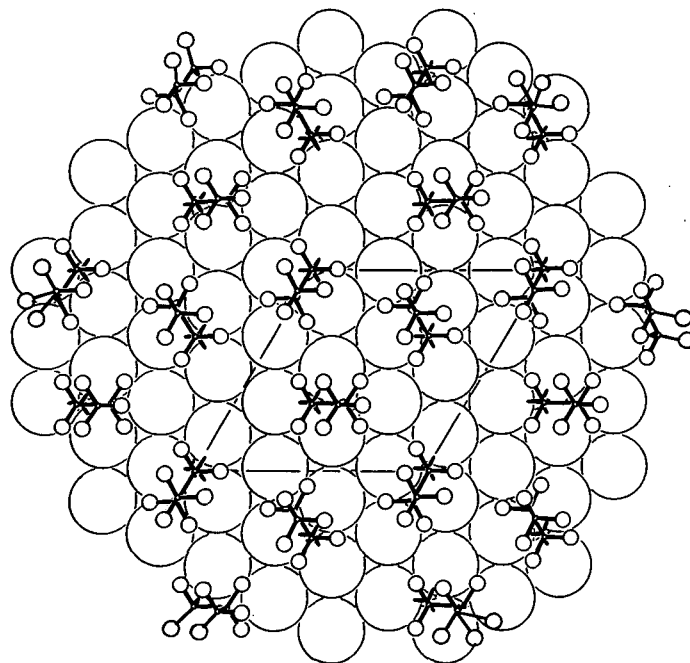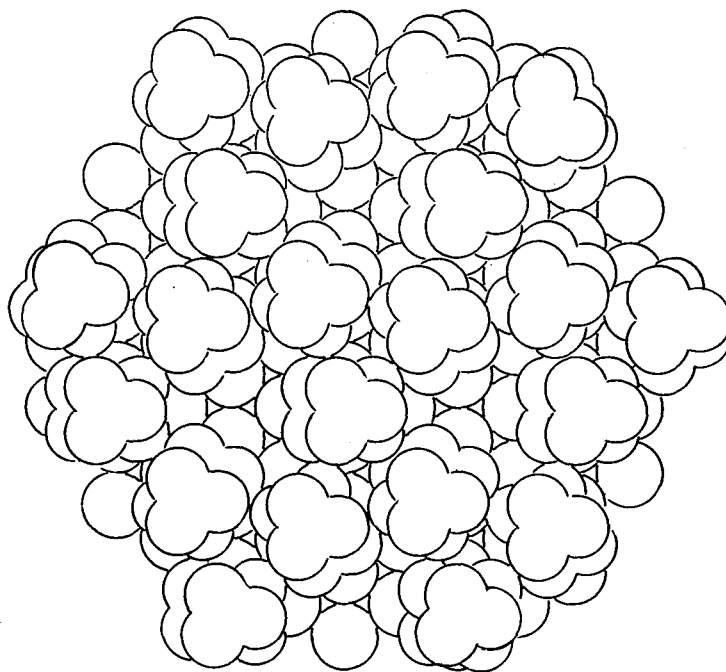
fcc(III) + $(2\sqrt{3} \times 2\sqrt{3})R30°$ $C_4H_7$ (butylidyne)

XBL 813-5411

Fig.12

Table 1.

| | $C_2H_2$ (acetylene) | $C_2H_4$ (ethylene) | cis- or trans-2-$C_4H_8$ (2-butenes) low exposure (10 L) | high exposure (~1000 L) | Intermediate exposure (~100 L) | $C_3H_4$ (methylacetylene) | $C_3H_6$ (propylene) |
|---|---|---|---|---|---|---|---|
| **METASTABLE SPECIES:** | | | | | | | |
| LEED pattern | (2x2) | disordered | disordered | | | (2x2) | disordered |
| proposed structure | parallel bonded di-σ, (~sp²) | parallel bonded di-σ (~sp³) | possibly parallel bonded di-σ (~sp³) | | | parallel bonded di-σ (sp²) extra methyl disordered | possibly parallel bonded di-σ (sp²) |
| techniques used | ELS, UPS | ELS, UPS | TDS | | | LEED (this work) | TDS |
| **CONVERSION TO STABLE SPECIES** | | | | | | | |
| temperature | 350 K | 280 K | 280 K | | | 350 K | 280 K |
| hydrogen needed? | yes | no | no | | | yes | no |
| **STABLE SPECIES:** | | | | | | | |
| LEED pattern | (2x2) | (2x2)[with e- beam] | diffuse (2√3x2√3)R30° | (2x√3x2√3)R30° | (8x8) | (2x2) | (2x2) |
| proposed structure | ethylidyne | ethylidyne | butylidyne extra ethyl randomly oriented | butylidyne extra ethyl locked in position | butylidyne | propylidyne extra methyl randomly oriented | propylidyne extra methyl randomly oriented |
| techniques used | LEED, ELS, TDS | LEED, ELS, TDS | LEED (this work), TDS | LEED (this work) | LEED (this work) | LEED (this work) | LEED (this work), TDS |
| **ALKYLIDYNE DECOMPOSITION TEMPERATURE:** | 450 K | 450 K | 325 K | 325 K | 325 K | 400 K | 400 K |

31